https://doi.org/10.46813/2026-161-055

UDC 621.315.592.3; 539.1.074.5

THE EFFECT OF SELENIUM ADDITIONS ON THE ELECTROPHYSICAL AND RECORDING PROPERTIES OF CdZnTe-BASED DETECTORS

O.I. Kondrik[1], D.O. Solopikhin[1,2]
[1]National Science Center "Kharkiv Institute of Physics and Technology", Kharkiv, Ukraine;
[2]Kharkiv National Automobile and Highway University, Kharkiv, Ukraine
E-mail: alex.kondrik2017@gmail.com

The results of quantitative investigations of the influence of impurities and structural defects content on the electrophysical and detector properties of $Cd_{0.9}Zn_{0.1}Te_{1-y}Se_y$, in particular $Cd_{0.9}Zn_{0.1}Te_{0.98}Se_{0.02}$ grown by the Bridgman method and $Cd_{0.9}Zn_{0.1}Te_{0.93}Se_{0.07}$ obtained by the heater traveling method, are highlighted. Studies have been carried out on the effect of defects on the change in resistivity ρ, free charge carrier concentration, Fermi level F, and charge collection efficiency η in radiation detectors based on CdZnTeSe:In at the temperature of 25°C. The dependences of the changes in ρ, *F*, and η on the content of impurities, cadmium vacancies and secondary tellurium phases were established. The conditions for maintaining the high-resistance state and response to irradiation in a detector based on $Cd_{0.9}Zn_{0.1}Te_{1-y}Se_y$ have been determined.

INTRODUCTION

Semiconductor radiation detectors operating at room temperature have applied in such areas as medical imaging, nuclear safety, nuclear non-proliferation control, astrophysics, high-energy physics, etc. [1–5]. The difficulty in developing new materials for such applications is explained by the stringent requirements to their properties. Although significant progress has been made in the development of alternative materials for radiation detectors, CdZnTe (CZT) has achieved the widest application, mainly due to its high energy resolution at room temperature. However, despite advances in CZT production technology [6], this compound has several problems: the Zn segregation coefficient ranges from 1.05 to 1.6 depending on the growth method and Zn content [7]; the formation of a large amount of crystalline defects, such as subgrain boundaries; a high concentration of tellurium inclusions [8]. Selenium additive to CZT has proven to be a very effective way to reduce the above-mentioned challenges [9 – 13]. The segregation coefficient of Se (k_{Se}) in the CdTe matrix is close to unity and this element affects the segregation coefficient of zinc k_{Zn} in CZT, changing it towards unity. That leads to better compositional homogeneity, as well as a reduction in the concentration of tellurium inclusions and improved charge transport properties [14, 15]. It is possible to obtain detector-grade CdZnTeSe (CZTS) material having a higher yield of a suitable product and, accordingly, potentially at a lower cost [16]. At the same time, the addition of Se to CdZnTe increases the lifetime of non-equilibrium charge carriers, electron mobility, and also enables for the adjustment of the band gap, which also makes it a promising candidate for use in ionizing radiation detectors [9, 12, 13, 17, 18].

The specifications of semiconductor detectors are significantly affected by structural defects, which form energy deep levels in the band gap, which act as centers for the capture and recombination of non-equilibrium charge carriers. One of such harmful structural defects in detector materials based on CdTe and CdZnTe are cadmium vacancies V_{Cd} and tellurium vacancies V_{Te} [19–21], which can significantly reduce the non-equilibrium charge carrier lifetime τ and the charge collection efficiency η. To compensate for charged acceptor defects, the dopants of shallow donors, such as In, Al [19, 22] are introduced. To reduce noise in the detector, its matrix must have a high resistivity of at least $\sim 10^{10}$ Ω·cm. That significantly complicates the experimental study of the influence of the i_{th} energy levels E_i in the band gap, their non-equilibrium charge carrier capture cross section σ_i and defect concentrations N_i on the lifetime of non-equilibrium electrons τ_e and holes τ_h, as well as on the detector charge collection efficiency and its resistivity ρ. Experimentally studied detector materials contain impurities and defects in fixed concentrations, which makes it impossible to determine their place in the overall picture of changes in electrophysical and detector properties. Quantitative model studies of ρ, μ_e τ_e τ_h and η using experimentally determined values E_i, σ_i, N_i make it possible to understand the mechanisms of change in the electrophysical and detector properties of CZTS-based materials depending on the characteristic parameters of impurities and defects, as well as to clarify the intervals of changes in their concentration within that a detector-quality semiconductor can be obtained. For a model study of the effects of selenium additives in CZTS on changes in the electrophysical and detector properties of these materials, a material that composition has been studied experimentally, i.e. with a known content of defects and parameters of their energy levels, should be taken as a basis.

The purpose of this work was to determine by computer modeling the optimal content of impurities and structural defects in CdZnTeSe, as well as the nature of their influence on the electrophysical and detector properties, based on the content of the

experimentally investigated materials $Cd_{0.9}Zn_{0.1}Te_{0.98}Se_{0.02}$ and $Cd_{0.9}Zn_{0.1}Te_{0.93}Se_{0.07}$, doped with indium.

THEORETICAL MODEL AND MATERIALS CONTENT

Model studies of CZTS were carried out using the values N_i, E_i, σ_i published in [20] as initial parameters. To simulate dynamic changes in material properties, physical and mathematical models were used, described in detail and tested for reliability in [23].

To determine the Fermi level *F* and the concentration of free charge carriers in the parabolic zone approximation, a multilevel compensation model was used for an arbitrary number of impurities and defects with the compilation and numerical solution of the corresponding electroneutrality equation. The electron mobility μ_e was calculated taking into account scattering mechanisms at ionized and neutral centers, and at acoustic, piezoelectric, and optical phonons. The hole mobility μ_p was assumed to be constant and equal to 70 $cm^2/(V \cdot s)$. The band gap width E_G in $Cd_{1-x}Z_xTe_{1-y}Se_y$ depending on the Se content was studied in [24] and, based on the results of this work, was calculated according to the formula:

$$E_G(x, y) = 1.511 - 0.54y + 0.6x. \quad (1)$$

The specific conductivity was calculated using the formula $en\mu_n + ep\mu_p$ (e – electron charge, *n* and *p* – concentrations of free electrons and holes, respectively). The specific resistance ρ was calculated as the reciprocal of the specific conductivity, consisting of the electron ($en\mu_n$) and hole ($ep\mu_p$) components. It follows from the results of the experiment on measuring the band-to-band recombination coefficients [25], that the rate of that recombination at room temperature in the wide-gap semiconductors under study is approximately by ten orders of magnitude lower than the rate of recombination at impurity and defect deep levels. Therefore, Shockley-Reed statistics were used to calculate the lifetimes of non-equilibrium electrons τ_e and holes τ_h. The charge collection efficiency of detector was determined by the Hecht equation [26, p. 489]. The distance between the electrodes of the flat detector was taken to be 5 mm, and the electric field voltage was 1000 V/cm.

The authors [20] identified point defects in the form of energy levels within the band gap of crystals in two types of detectors based on CdZnTeSe grown by the Bridgman Method (BM) and the Traveling Heater Method (THM). These energy levels, measured experimentally, are presented in Table. The values of the capture cross section σ_i of non-equilibrium charge carriers by defect levels given there were determined using the DLTS (deep level transient spectroscopy) technique and they were used in the simulation for all levels except the trap E_C – 0.78 eV. For it, the σ value was adopted, which corresponded to the data obtained from the results of the experimental method TSC (Thermally Stimulated Current), published in a number of papers, for example, in [27]. TSC spectra are usually processed using the SIMPA (Simultaneous Multiple Peak Analysis) fitting technique, which is used to measure capture cross sections, when the contribution of all levels to the emission of charge carriers into the corresponding zones is simultaneously taken into account. Such data make it possible to correctly use the Shockley-Reed model to calculate τ_e and τ_h properly.

Content of traps in $Cd_{0.9}Zn_{0.1}Te_{0.98}Se_{0.02}$ (BM) and $CdTe_{0.93}Se_{0.07}$ (THM)

Concentration, cm^{-3} (obtaining methods)		Energy levels E_i, eV	σ_i, cm^2	Origin of the trap [20]
$Cd_{0.9}Zn_{0.1}Te_{0.98}Se_{0.02}$ (BM)	$Cd_{0.9}Zn_{0.1}Te_{0.93}Se_{0.07}$ (THM)			
$5 \cdot 10^{12} \ldots 1 \cdot 10^{14}$	$2 \cdot 10^{12} \ldots 2 \cdot 10^{13}$	E_C – 0.014	$1.6 \cdot 10^{-22}$	Impurity In_{Cd}
$6 \cdot 10^{10}$	$6 \cdot 10^{10}$	E_C – 0.022	$9 \cdot 10^{-21}$	Donor impurity
$5 \cdot 10^{10}$	$5 \cdot 10^{10}$	E_C – 0.058	$5 \cdot 10^{-17}$	Se-related donor
$1 \cdot 10^{11}$	$1.3 \cdot 10^{11}$	E_V + 0.18	$1 \cdot 10^{-16}$	A-center
$2 \cdot 10^{10}$	$2 \cdot 10^{11}$	E_V + 0.26	$1 \cdot 10^{-14}$	Te_i – interstitial
$4 \cdot 10^{10}$	0	E_V + 0.37	$1 \cdot 10^{-15}$	Cd vacansy: V_{Cd}^-
0	$4 \cdot 10^{10}$	E_C –0.78	$5 \cdot 10^{-11}$	Te_{Cd}^{++}
$4 \cdot 10^{11}$	0	E_V + 1.1	$1 \cdot 10^{-10}$	Tellurium secondary phases Te_{SP}

It should be noted that when processing TSC spectra by the SIMPA method, the contribution of the dark current $I_{dark}(T)$ is taken into account, which has the form: $I_{dark}(T) = Ce^{\frac{E_{DD}}{kT}}$, where C is a constant, E_{DD} is the deep donor level, *k* is the Boltzmann constant, and *T* is the temperature. A deep donor with E_{DD} energy ensures a high-resistive state of the materials under study. It was established in our work that these deep donors have the energy $E_{DD} = E_C - 0.860$ eV and concentration $N_{DD} = 6 \cdot 10^{10}$ cm^{-3} for the material grown by the Bridgman method, as well as $E_{DD} = 0.833$ eV and $N_{DD} = 2 \cdot 10^{11}$ cm^{-3} for the material obtained by the THM method. In the experiment [20], materials with constant concentrations of impurities and defects were grown. It is of interest to comprehensively investigate the behavior of ρ depending on the content of tellurium secondary phases Te_{SP}, doping In, and the deep traps of V_{Cd} and the tellurium interstitial Te_i in wide intervals of changes in their concentrations.

RESULTS AND DISCUSSION

For effective registration of ionizing radiation by a detector, it is necessary that the resistivity ρ of the detector material be at least 10^{10} Ω·cm. Authors of paper [20] were obtained the two semiconductor materials:

$Cd_{0.9}Zn_{0.1}Te_{0.98}Se_{0.02}$ – CZTS (BM) possessing the resistivity $\rho = 1\cdot10^{10}$ Ω·cm and $Cd_{0.9}Zn_{0.1}Te_{0.93}Se_{0.07}$ – CZTS (THM) with $\rho = 2\cdot10^{9}$ Ω·cm. It should be noted that the resistivity values of 10^{10} Ω·cm measured in [20] were in full agreement with the values of ρ for CZTS (BM) calculated according to the adopted model, where the N_i concentrations and energy levels E_i determined by the DLTS method served as the initial parameters. In contrast, when substituting the measured values N_i and E_i for the CZTS (THM) sample into the modeling program, a low-resistance state of ~ 10^4 Ω·cm was obtained. As it is known, the high-resistance state of CdTe and CdZnTe (10^9…10^{10} Ω·cm) leads to significant difficulties when attempting to accurately determine their defect concentrations. It is likely such an inaccuracy occurred for the E_C – 0.022 and E_C – 0.058 eV levels, which were represented in amounts of $4\cdot10^{11}$ and $3\cdot10^{11}$ cm^{-3}, respectively, that is about by an order of magnitude higher than for the CZTS (BM) material. Reducing their content by approximately an order of magnitude (see table) led to complete agreement between the measured $\rho=2\cdot10^{9}$ Ω·cm and the calculated model resistivity values. On the other hand, comparing the ρ values of the two materials, it can be argued that $Cd_{0.9}Zn_{0.1}Te_{0.98}Se_{0.02}$, grown by the Bridgman method, is more suitable for recording X-ray and γ-radiation. According to the authors, the one-order higher resistivity of $Cd_{0.9}Zn_{0.1}Te_{0.98}Se_{0.02}$ is explained by the higher concentration of secondary tellurium phases in it.

Fig. 1 shows the behavior of the resistivity as a function of the concentration of doping indium and the content of cadmium vacancies V_{Cd} (a) and the secondary tellurium phase (b) for $Cd_{0.9}Zn_{0.1}Te_{0.98}Se_{0.02}$ grown by the Bridgman method. It can be seen from Fig. 1 that with increasing V_{Cd} concentration, ρ decreases, while with changing content of secondary phases of tellurium Te_{SP} the resistivity does not change. In other words, the resistivity does not depend at all on the content of tellurium precipitates at any concentration of doping indium. This result can be explained by the fact that the acceptor energy level E_V+1.1 eV of Te_{SP} in the high-resistance state is located significantly above the Fermi level. Therefore, it always lacks trapped electrons that could move between atoms, contributing to the hole current. For this reason, this level has no effect on the resistivity. It should be noted that in the majority of works investigating materials based on CdZnTe, this energy level is attributed to the donor defect V_{Te} or Te_{SP} with the energy $E_{DD} = E_C - 1.1$ eV. However, even in this case, the resistivity should also not depend on the content of this defect, because the Fermi level *F* is much higher than the E_{DD} energy level, which remains neutral in the high-resistance state and does not give electrons to the conduction band and, thus, does not affect the conductivity of the material.

This contradicts the conclusion of the authors [20], who believe that the smaller value of $\rho=2\cdot10^{9}$ Ω·cm for $Cd_{0.9}Zn_{0.1}Te_{0.93}Se_{0.07}$ compared to $\rho=(1\ldots2)\cdot10^{10}$ Ω·cm для $Cd_{0.9}Zn_{0.1}Te_{0.98}Se_{0.02}$ is explained by the presence of Te_{SP} in the last in the amount of $4\cdot10^{11}$ cm^{-3} (see Table). In our opinion, the smaller value of ρ for $Cd_{0.9}Zn_{0.1}Te_{0.93}Se_{0.07}$ is explained more simply, namely by the smaller width of the band gap E_G, which according to formula (1) for this material is equal to 1.533 eV, which is less than 1.560 eV for $Cd_{0.9}Zn_{0.1}Te_{0.98}Se_{0.02}$. That is, the smaller value of ρ is determined by the larger amount of selenium additive.

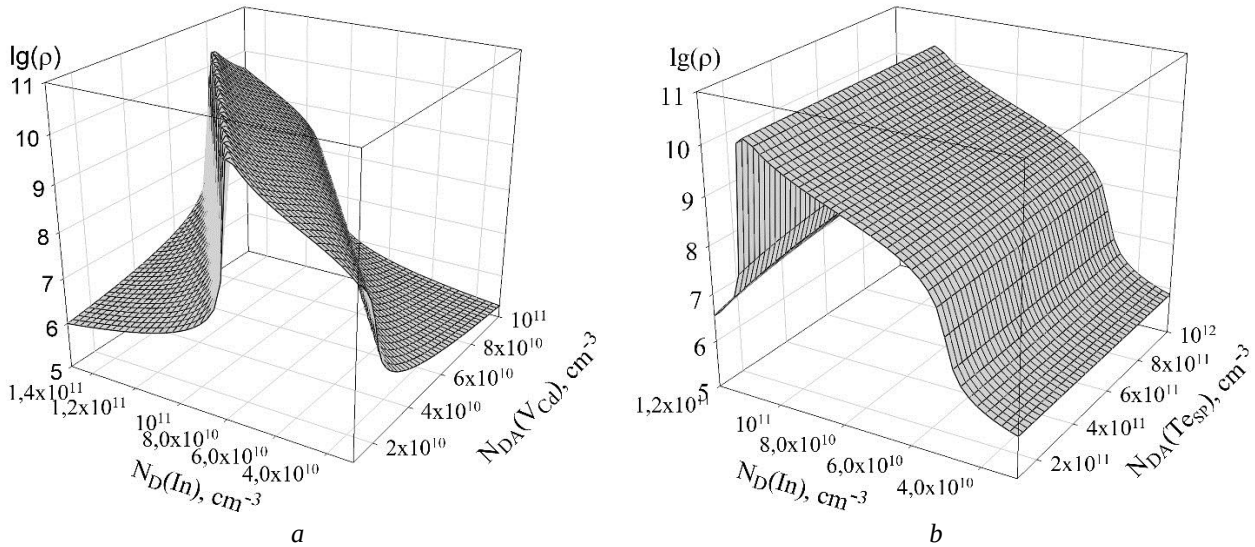

Fig. 1. Dependences of the decimal logarithm of the resistivity on the content of indium and cadmium vacancies (a), as well as indium and tellurium vacancies (b) for $Cd_{0.9}Zn_{0.1}Te_{0.98}Se_{0.02}$

Fig. 2 shows the change in the Fermi level *F* in $Cd_{0.9}Zn_{0.1}Te_{0.98}Se_{0.02}$ as a function of the concentrations of indium impurity and secondary phases (precipitations) of tellurium. The wide inclined plane that crosses the middle of the band gap refers to the high-resistance state of this material.

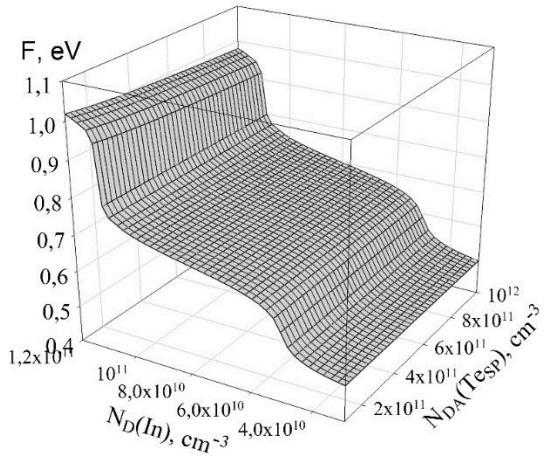

Fig. 2. Behavior of the Fermi level F for $Cd_{0.9}Zn_{0.1}Te_{0.98}Se_{0.02}$(BM) depending on the content of doping indium and the tellurium secondary phases

Further comparison of the electrophysical properties of CZTS(BM) and CZTS(THM) will be carried out by the content of the interstitial tellurium defect Te_i, which is present in both detector materials under study. Fig. 3 shows the dependencies ρ[N(In), N(Te_i)] for $Cd_{0.9}Zn_{0.1}Te_{0.98}Se_{0.02}$ (BM) *(a)* and $Cd_{0.9}Zn_{0.1}Te_{0.93}Se_{0.07}$ (THM) (*b*). The value of the band gap for calculating the resistivity of $Cd_{0.9}Zn_{0.1}Te_{0.93}Se_{0.07}$ (THM) was taken to be 1.43 eV to agree with the experimental results of measuring ρ.

Both dependencies are characterized by extended resistivity maxima, which the conditions of mutual compensation of acceptor defects Te_i and donor impurities of doping indium are fulfilled for. The same behavior is characteristic of the extended resistivity maximum in Fig. 1,a, where the ionized acceptor cadmium vacancies are compensated by impurities of the shallow indium donor. However, despite the fact that a signal was recorded in CZTS (THM), unlike CZTS (BM), the detector based on it is not suitable for ionizing radiation spectroscopy due to the low resistivity ($2 \cdot 10^9$ Ω·cm) and, as a result, large noise in the pulse height spectra.

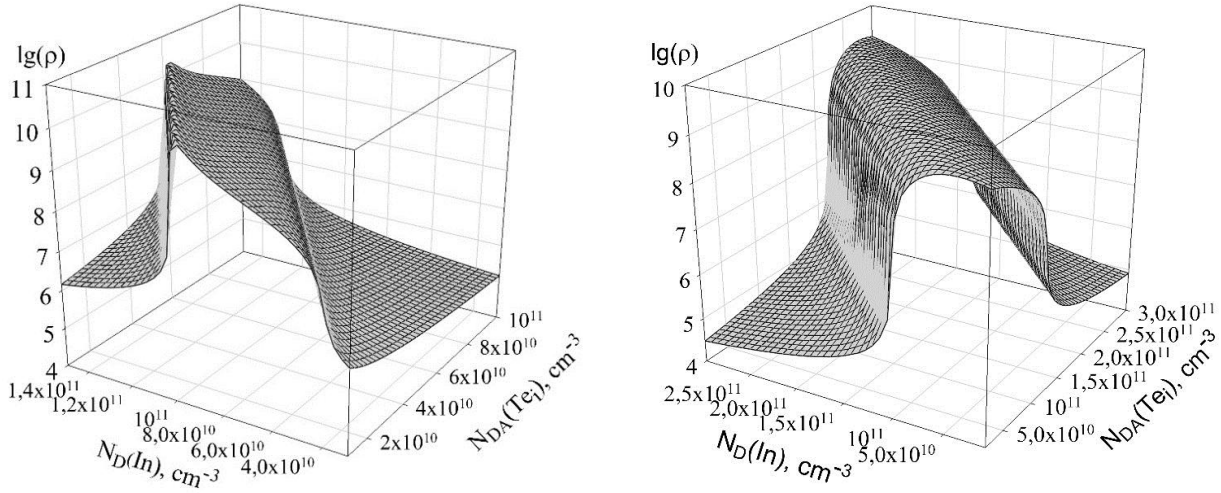

a *b*

Fig. 3. Dependences of the decimal logarithm of resistivity on the concentration of indium and interstitial tellurium for $Cd_{0.9}Zn_{0.1}Te_{0.98}Se_{0.02}$ (a) and $Cd_{0.9}Zn_{0.1}Te_{0.93}Se_{0.07}$ (b)

Model calculations of the resistivity depending on the concentration of doping indium were performed for different selenium contents (Fig. 4).

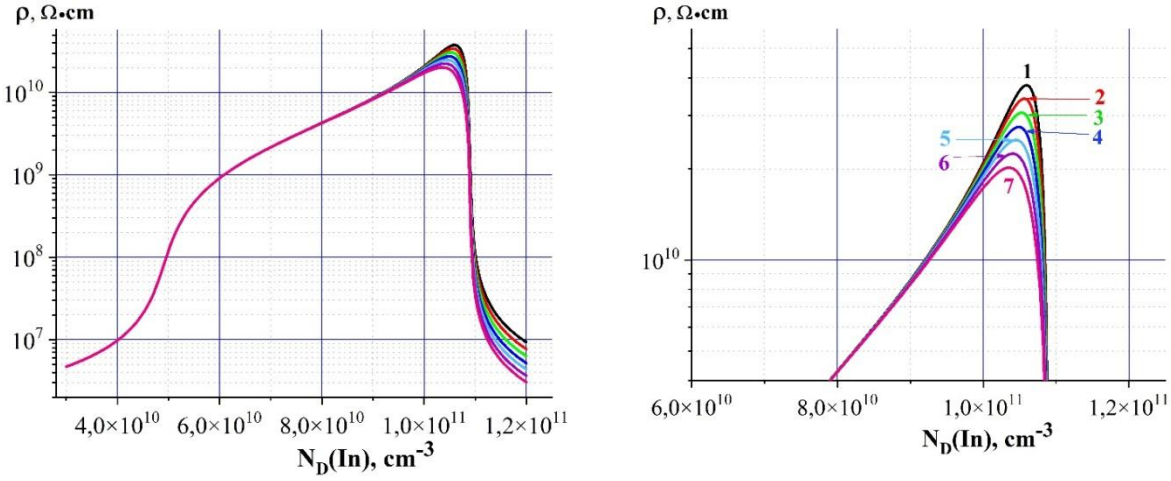

a *b*

Fig. 4. Dependences of the resistivity of $Cd_{0.9}Zn_{0.1}Te_{1-y}Se_y$ on the concentration of doping indium at the temperature 25 °C and different selenium contents, y: 1 – 0.01, 2 – 0.02, 3 – 0.03, 4 – 0.04, 5 – 0.05, 6 – 0.06, 7 – 0.07, in the entire studied range (a); in the high-resistance state (b)

The dependences in Fig. 4 were calculated for the initial defect composition of the CZTS(BM) sample, but for different selenium additions varying within the range $0.01 \le y \le 0.07$. The band gap E_G for various Se additives was calculated using formula (1) and gradually decreased from 1.5656 eV for y=0.01 to 1.533 eV for y=0.07. Fig, 4,a demonstrates the behavior of ρ over the entire studied range of changes in the concentration of the indium dopant. In Fig. 4,b shows only the upper, high-resistance part of the dependences, where the differences between the curves are noticeable. In the lower part of the graph, the dependencies almost coincide. In addition, it can be seen that the maximum ρ values for all *y* magnitudes are above 10^{10} Ω·cm and vary from ~$3.8\cdot10^{10}$ for y=0.01 to $2\cdot10^{10}$ Ω·cm for y = 0.07. This result of model calculations contradicts a number of experimental results that resistivity decreases noticeably with an increase in the selenium content to 0.07 at.%.

For example, it is reported in [28] that for $Cd_{0.9}Zn_{0.1}Te_{1-y}Se_y$, when selenium was added in amounts of y = 0.015 and 0.02, a material with ρ = $(1\ldots3)\cdot10^{10}$ Ω·cm was obtained, and at y = 0.04 ρ = $1\cdot10^{10}$, and also at *y* = 0.07 the resistivity was already within $(2\ldots5)\cdot10^{9}$ Ω·cm. Moreover, in $Cd_{0.9}Zn_{0.1}Te_{0.98}Se_{0.02}$, a signal was recorded with the high energy resolution of 0.77% of the main peak at 662 keV from the ^{241}Am source (measured without charge loss correction algorithms) at room temperature [12]. On the other hand, the calculations of resistivity change dependencies were carried out using classical, proven models, so their discrepancies with the experiment can be explained as follows. It is likely that an increase in the selenium content leads to the ingress of its atoms into the interstitial spaces, with the subsequent appearance of secondary Se phases, which can form throughout the entire volume of the CZTS crystal. As is known, selenium exists in various allotropic modifications, including in the form of a crystalline hexagonal structure, which has a resistivity of ~ 10^6 Ω·cm [29] that is significantly less than the value of ~10^{10} Ω·cm for $Cd_{0.9}Zn_{0.1}Te$. Therefore, when measuring ρ, the current passes not only through the basic crystal, but also through the selenium secondary phases which are limited by certain boundaries. Thus, a kind of shunting of CdZnTeSe matrix occurs and the measured resistance decreases.

It is of interest to investigate and clarify the specific reasons for the degradation of the detector properties of $Cd_{0.9}Zn_{0.1}Te_{0.98}Se_{0.02}$ (BM). The processes of capture and recombination of non-equilibrium electrons, which mainly form the signal in the pulse height spectrum, are determined by deep levels of acceptor defects. Comparing the content of both materials (see table), we can see that the main difference between them is the presence of two acceptor defects: cadmium vacancies and secondary tellurium phases Te_{SP} in CZTS (BM). Thus, it is necessary to perform model calculations of the charge collection efficiency η in the detector depending on the V_{Cd} and Te_{SP} content. As a result of modeling studies, it was found that in a detector based on CZTS(BM), the signal is reliably recorded at $N(E_V+1.1) = 4\cdot10^{10}$ cm^{-3} and $\sigma(E_V+1.1) = 1\cdot10^{-9}\ldots1\cdot10^{-10}$ cm^2. The characteristics of the remaining levels are shown in the table, and the capture cross section $\sigma(E_V+1.1)$ is taken to be even larger: $3\cdot10^{-9}$ cm^2. The simulation result is shown in Fig. 5 which demonstrates the behavior of η in a flat detector depending on the concentration of doping indium for different cadmium vacancy contents. It can be seen from Fig. 5, that changing the V_{Cd} content does not affect the maximum charge collection value, but only shifts the η(In) curves when $N(V_{Cd})$ changes, and the width of the high-resistance region does not alter. So, you can always choose the concentration of indium to get the maximum signal amplitude.

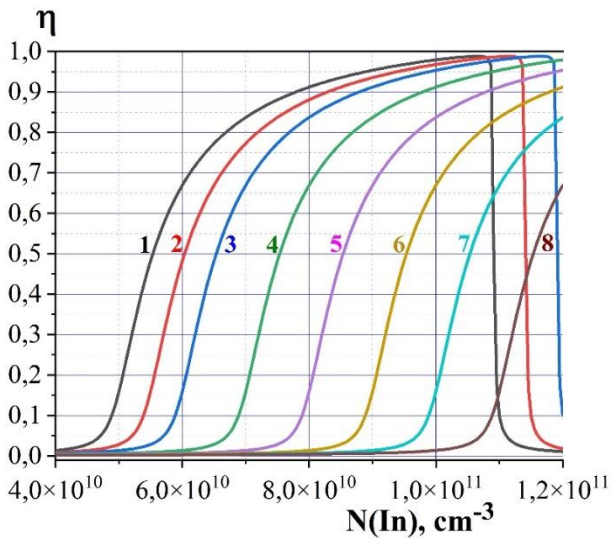

Fig. 5. Dependences of charge collection efficiency η on the indium content at different concentrations of cadmium vacancies, cm^{-3}: 1 – $4\cdot10^{10}$; 2 – $4.5\cdot10^{10}$; 3 – $5\cdot10^{10}$; 4 – $6\cdot10^{10}$; 5 – $7\cdot10^{10}$; 6 – $8\cdot10^{10}$; 7 – $9\cdot10^{10}$; 8 – $1\cdot10^{11}$

The simulation also showed that the resistivity correlates with the value of charge collection: the larger ρ, the larger the magnitude of η. Therefore, at maximum charge collection, a high-resistance detector material with minimal leakage currents and low noise in the spectrum should be obtained.

Thus, it can be assumed that the complete degradation of the registration properties of the CZTS (BM) detector recorded by the authors [20] is somehow related to the Te secondary phases. Before performing model studies of the influence of the content of secondary phases Te_{SP} in the matrix on the signal magnitude, certain features of these defects should be taken into account. Tellurium secondary phases can be quite large (over 30 μm) and very extended [20], and an increase in their measured concentration is probably accompanied by an increase in their size. The increase in size necessarily causes a decrease in the average drift length of charge carriers, primarily non-equilibrium electrons caused by irradiation with gamma quanta from a radioactive source. As the size of these defects increases, the frequency of their capture of non-equilibrium charge carriers should also increase. That is, it is quite likely that such an important characteristic as the capture cross section of non-equilibrium charge carriers increases. We assume that the position of the

Te_{SP} energy level remains unchanged or changes slightly. The result of model studies taking into account the described assumptions is presented in Fig. 6, where in addition to the dependences η(In) (left vertical axis), the dependence of the resistivity on the indium content (right vertical axis) is also shown, which is the same for all variable parameters that determine different η curves.

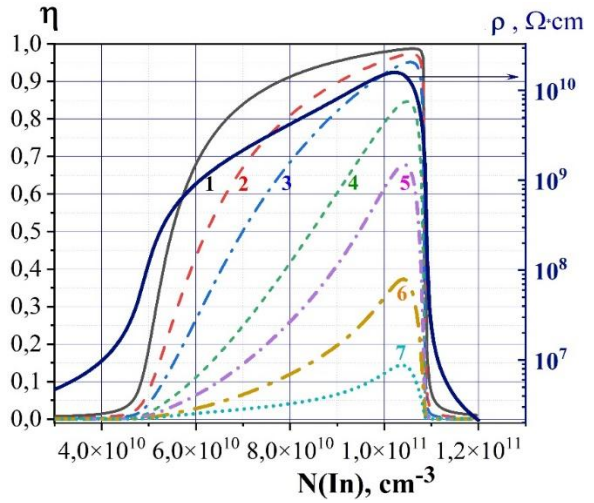

Fig. 6. Dependences of charge collection efficiency and resistivity of a CZTS(BM)-based detector on the indium concentration for different concentration values Te_{SP}, cm^{-3}: 1 – $4\cdot10^{10}$; 2 – $8\cdot10^{10}$; 3 – $1\cdot10^{11}$; 4 – $2\cdot10^{11}$; 5 – $3\cdot10^{11}$; 6 – $3.5\cdot10^{11}$; 7 – $4\cdot10^{11}$

That demonstrates the fairly good correlation between the values of η and ρ mentioned above. The Te_{SP} concentration varies from $4\cdot10^{10}$ cm^{-3} to the value $4\cdot10^{11}$ cm^{-3} recorded in the experiment [20]. The capture cross section σ gradually increases from $1\cdot10^{-11}$ cm^2 (for dependence 1) to the value $\sigma = 1\cdot10^{-10}$ cm^2 (for dependence 7) measured in the experiment [20]. In addition, the drift length d, measured from the anode, for non-equilibrium electrons gradually decreases from d = 4.9 (curve 1) to d = 0.1 mm (curve 7). Since modern experimental research methods are not yet able to determine accurately the characteristics of defects in high-resistance materials, then all results of model calculations based on experimental data can only be of a qualitative nature. It can be seen from Fig. 6 that the charge collection efficiency decreases markedly with an increase in the content and size of the particles of the tellurium secondary phase and, accordingly, with a decrease in the drift length of non-equilibrium charge carriers, while maintaining the concentrations of the remaining defects given in the table unchanged.

The model calculations of the electron mobility μ_e and the lifetime of nonequilibrium electrons τ_e were also carried out for the studied $Cd_{0.9}Zn_{0.1}Te_{1-y}Se_y$ materials provided that there are no precipitates or secondary phases in their matrix. As a result, it turned out that in ideally homogeneous materials $\mu_e = 970$ $cm^2/(V\cdot s)$, $\mu_e\cdot\tau_e = 9\cdot10^{-3}$ cm^2/V. In the experiments described in [28], the $Cd_{0.9}Zn_{0.1}Te_{1-y}Se_y$-based ($0.015 < y < 0.07$) samples were obtained, and measured values of $\mu_e\cdot\tau_e$ turned out within the range of $(1\ldots6.6)\cdot10^{-3}$ cm^2/V.

Increasing the size of secondary phases should affect drift and electron mobility in detector materials. Studies have been performed on the effect of electron mobility on the resistivity of CZTS (BM). To do this, the capture cross section of secondary phase clusters was increased from $1\cdot10^{-6}$ to $8\cdot10^{-5}$ cm^2. At the same time, the electron mobility μ_e decreased from 1023 to 420 $cm^2/(V\cdot s)$. As a result, it was found that the maximum resistivity increases slightly, namely from $2.7\cdot10^{10}$ to $4.25\cdot10^{10}$ Ω·cm, that is, only by one and a half times. Note that a material with μe = 420 cm2/(V·s) is not suitable for creating ionizing radiation detectors at all.

CONCLUSIONS

The main reason for the significant decrease and complete degradation of the signal in the detector based on $Cd_{0.9}Zn_{0.1}Te_{1-y}Se_y$ is the increase in the content and size of the particles of the secondary tellurium phase, which reduce the average drift length of non-equilibrium charge carriers within the interelectrode gap.

The main reason for the higher resistivity ρ for $Cd_{0.9}Zn_{0.1}Te_{0.98}Se_{0.02}$ grown by the Bridgman method compared to $Cd_{0.9}Zn_{0.1}Te_{0.93}Se_{0.07}$ obtained by the moving heater method is the addition of a smaller amount of selenium to it, but not the presence of secondary tellurium phases Te_{SP} in it. The addition of selenium to the CdZnTe matrix in an amount of up to 0.07 at. % leads to the formation of interstitial Se atoms with the subsequent formation of its secondary phases which have a lower resistivity. It leads to a decrease in the resistivity of the entire detector material and, as a result, an increase in leakage currents in the detector based on $Cd_{0.1}Zn_{0.9}Te_{1-y}Se_y$. It is desirable that the selenium content does not exceed 0.04% to preserve the detector quality of the material.

The resistivity value depends little on the content of interstitial tellurium and Te_{SP} due to the large difference between the energy levels of this defects and the Fermi level in the high-resistance state of CZTS (BM). A reduction in electron mobility of more than two times has little effect on the resistivity of the detector material.

An increase in the content of cadmium vacancies does not lead to a decrease in the maximum value of the charge collection efficiency η, but only to a shift in the dependences of η on the concentration of doping In.

REFERENCES

1. Henric S. Krawczynski, Daniel Stern, Fiona A. Harrisonet, et al. X-ray polarimetry with the Polarization Spectroscopic Telescope Array (PolSTAR) // *Astroparticle Physics*. 2016, v. 75, p. 8-28; https://doi.org/10.1016/j.astropartphys.2015.10.009

2. Piotr J. Slomka, Robert J.H. Miller, Lien-Hsin Hu, et al. Solid-state detector SPECT myocardial perfusion imaging // *J. Nucl. Med.* 2020, v. 60, issue 9, p. 1194-1204;
https://doi.org/10.2967/jnumed.118.220657

3. W. Jing and L. Chi. Recent advances in cardiac SPECT instrumentation and imaging methods // *Physics in Medicine and Biology*. 2019, v. 64, p. 06TR01; https://doi.org/10.1088/1361-6560/ab04de

4. J. Franc et al. Microhardness study of $Cd_{1-x}Zn_xTe_{1-y}Se_y$ crystals for X-ray and gamma ray detectors // *Materials Today Communications*. 2020, v. 24, issue 6, p. 101014;
http://dx.doi.org/10.1016/j.mtcomm.2020.101014

5. R. Nag. Growth. Characterization and Evaluation of CdZnTeSe Single Crystals for Room Temperature Radiation Detectors // *Master's thesis*. 2022; https://scholarcommons.sc.edu/etd/6781

6. A.E. Bolotnikov, G.S. Camarda, E. Chen, et al. Use of the drift-time method to measure the electron lifetime in long-drift-length CdZnTe detectors // *J. Appl. Phys*. 2016, v. 120, issue 10, p. 104507;
https://doi.org/10.1063/1.4962540

7. K. Kim, A.E. Bolotnikov, G.S. Camarda, et al. Overcoming Zn segregation in CdZnTe with the temperature gradient annealing // *J. Cryst. Growth*. 2016, v. 442, p. 98-101;
https://doi.org/10.1016/j.jcrysgro.2016.02.038

8. A.E. Bolotnikov, S. Babalola, G.S. Camarda, et al. Correlations between crystal defects and performance of CdZnTe detectors // *IEEE Trans. Nucl. Sci.* 2011, v. 58, issue 4, p. 1972-1980;
https://doi.org/10.1109/TNS.2011.2160283

9. Sandeep K. Chaudhuri, Joshua W. Kleppinger, OmerFaruk Karadavut, et al. Quaternary Semiconductor $Cd_{1-x}ZnxTe_{1-y}Se_y$ for High-Resolution, Room-Temperature Gamma-Ray Detection // *Crystals*. 2021, v. 11, p. 827; https://doi.org/10.3390/cryst11070827

10. Utpal N. Roy, Giuseppe S. Camarda, Yonggang Cui, et al. Evaluation of CdZnTeSe as a high-quality gamma-ray spectroscopic material with better compositional homogeneity and reduced defects // *Scientific Reports*. 2019, v. 9, Article number 7303; https://doi.org/10.1038/s41598-019-43778-3

11. M.L. Drabo, S.U. Egarievwe, U.N. Roy, et al. Study of CdZnTeSe gamma-ray detector under various bias voltages // *Materials Sciences and Applications*. 2020, v. 11, issue 8, p. 553-559;
https://doi.org/10.4236/msa.2020.118036

12. Utpal N. Roy, Giuseppe S. Camarda, Yonggang Cui et al. Impact of selenium addition to the cadmium‐zinc‐telluride matrix for producing high energy resolution X‐ and gamma-ray detectors // *Scientific Reports*. 2021, v. 11, Article number 10338; https://doi.org/10.1038/s41598-021-89795-z

13. U.N. Roy, G.S. Camarda, Y. Cui, R.B. James. Advances in CdZnTeSe for radiation detector applications // *Radiation*. 2021, v. 1(2), p. 123-130; https://doi.org/10.3390/radiation1020011

14. S.K. Chaudhuri, M. Sajjad, J.W. Kleppinger, K.C. Mandal. Charge transport properties in CdZnTeSe semiconductor room-temperature γ-ray detectors // *J. Appl. Phys*. 2020, v. 127, issue 24, p. 245706; https://doi.org/10.1063/5.0006227

15. J. Pipek, M. Betušiak, E. Belas, et al. Charge Transport and Space-Charge Formation in $Cd_{1-x}ZnxTe_{1-y}Sey$ Radiation Detectors // *Physical Review Applied*. 2021, v. 15, p. 054058;
https://doi.org/10.1103/PhysRevApplied.15.054058

16. U.N. Roy, G.S. Camarda, Y. Cui, and R.B. James. High-Resolution virtual frisch grid gamma-Ray detectors based on as-grown CdZnTeSe with reduced defects // *Appl. Phys. Lett*. 2019, v. 114, issue 23, p. 232107; https://doi.org/10.1063/1.5109119

17. Ezekiel O. Agbalagba, Mebougna L. Drabo, Stephen U. Egarievwe. Characterization of CdZnTeSe Nuclear Detector Chemically Etched in Bromine Methanol // *Materials Sciences and Applications*. 2021, v. 12, N 8, p. 363-373;
https://doi.org/10.4236/msa.2021.128025c

18. K. Kim, Y. Kim, F. Jan, P. Fochuk, et al. Enhanced hole mobility-lifetime product in selenium-added CdTe compounds // *Nuclear Instruments and Methods in Physics Research Section A: Accelerators, Spectrometers, Detectors and Associated Equipment*. 2023, v. 1053, p. 168363;
https://doi.org/10.1016/j.nima.2023.168363

19. S. R. Kavanagh, A. Walsh, D. O. Scanlon. Rapid Recombination by Cadmium Vacancies in CdTe // *ACS Energy Letters*. 2021, v. 6, issue 4, p. 1392-1398; https://doi.org/10.1021/acsenergylett.1c00380

20. R. Gul, U.N. Roy, G.S. Camarda, et al. A comparison of point defects in $Cd_{1-x}Zn_xTe_{1-y}Se_y$ crystals grown by Bridgman and traveling heater methods // *J. Appl. Phys*. 2017, v. 121, p. 125705; https://doi.org/10.1063/1.4979012

21. A.I. Kondrik. Degradation Mechanisms of the Detector Properties of CdTe and CdZnTe Under the Influence of Gamma Irradiation // *East European Journal of Physics*. 2021, N 3;
https://doi.org/10.26565/2312-4334-2021-3-18

22. A. Wardak, D.M. Kochanowska, M. Kochański, et al. Effect of doping and annealing on resistivity, mobility-lifetime product, and detector response of (Cd,Mn)Te // *Journal of Alloys and Compounds*. 2023, v. 936, p. 168280;
https://doi.org/10.1016/j.jallcom.2022.168280

23. A. Kondrik, G. Kovtun. Influence of impurities and structural defects on electrophysical and detector properties of CdTe and CdZnTe // *Tekhnologiya i konstruirovanie v elektronnoi apparature*. 2019, N 5-6 (in Russian); https://doi.org/10.15222/TKEA2019.5-6.43

24. G. Brill, Y. Chen, P.M. Amirtharaj, et al. Molecular Beam Epitaxial Growth and Characterization of Cd-Based II–VI Wide-Bandgap Compounds on Si Substrates // *J. Electron. Mater*. 2005, v. 34, p. 655-661; https://doi.org/10.1007/s11664-005-0080-y

25. G.F. Novikov, N.A. Radychev. Experimental determination of the dependence of the free electron-hole recombination rate constant on the band gap in semiconductors of the $A^{II}B^{VI}$ and $A^{I}BV^{II}$ types // *Russ. Chem. Bull*. 2007, v. 56, p. 890-894;
https://doi.org/10.1007/s11172-007-0134-9

26. Glenn F. Knoll. Radiation Detection and Measurement, 4th edition // *John Wiley & Sons, Inc.* 2010, 829 p.

27. Lingyan Xu, Tao Feng, Wanqi Jie. Defect levels characterized by photoconductivity and thermally stimulated current in CdZnTe crystals // *Journal of Crystal Growth.* 2021, v. 560-561, p. 126050;
https://doi.org/10.1016/j.jcrysgro.2021.12605

28. U.N. Roy, G.S. Camarda, Yonggang Cui, and R.B. James. Optimization of selenium in CdZnTeSe

quaternary compound for radiation detector application // *Appl. Phys. Lett*. 2021, v. 118, p. 152101; https://doi.org/10.1063/5.0048875

29. T. Moss. *Optical Properties of Semiconductors*. M., 1961, 304 p.

Article received 16.10.2025

ВПЛИВ ДОБАВОК СЕЛЕНУ НА ЕЛЕКТРОФІЗИЧНІ ТА РЕЄСТРУВАЛЬНІ ВЛАСТИВОСТІ ДЕТЕКТОРІВ НА ОСНОВІ CdZnTe

О.І. Кондрик, Д.О. Солопіхін

Висвітлено результати кількісних досліджень впливу вмісту домішок та структурних дефектів на електрофізичні та детекторні властивості $Cd_{0.9}Zn_{0.1}Te_{1-y}Se_y$, зокрема $Cd_{0.9}Zn_{0.1}Te_{0.98}Se_{0.02}$, вирощеному методом Бріджмена, і $Cd_{0.9}Zn_{0.1}Te_{0.93}Se_{0.07}$, одержаному методом пересувного нагрівача. Виконано дослідження впливу дефектів на зміну питомого опору ρ, концентрації вільних носіїв заряду, рівня Фермі *F* та ефективності збору зарядів η у детекторах випромінювань на основі CdZnTeSe:In при температурі 25 °C. Встановлено залежності змін ρ, *F*, η від вмісту домішок, вакансій кадмію і вторинних фаз телуру. Визначено умови збереження високоомного стану та відгуку на опромінення в детекторі на основі $Cd_{0.9}Zn_{0.1}Te_{1-y}Se_y$.